Pergamon

Int. J. Heat Mass Transfer. Vol. 38, No. 3, pp. 519–531, 1995

0017-9310/95 $9.50+0.00

0017-9310(94)00123-5

Free stream cooling of a stack of parallel plates

A. M. MOREGA,† A. BEJAN†‡ and S. W. LEE¶

†Department of Mechanical Engineering and Materials Science, Duke University, Durham, NC 27708-0300, U.S.A. and ¶Mechanical Technology Department, IBM NS, Research Triangle Park, NC 27709, U.S.A.

(*Received* 1 *July* 1993 *and in final form* 18 *April* 1994)

Abstract—This paper addresses the fundamental heat transfer augmentation question of how to arrange a stack of parallel plates (e.g. fins of heat sink, printed circuit boards) in a free stream such that the thermal resistance between the stack and the stream is minimum. It is shown that the best way of positioning the plates relative to one another is by spacing them equidistantly. When the overall dimensions of the stack are specified, there is an optimal number of plates for minimum thermal resistance. The optimal number and minimum resistance are anticipated theoretically and correlated into compact formulas that agree with numerical and experimental results in the Re_L range 10^2–10^4. Finally, it is shown that a stack with more plates than the optimal number can be modeled more expediently as a porous block immersed in a free stream.

1. INTRODUCTION

In this paper we consider a fundamental problem of heat transfer augmentation, which has important applications in the area of electronic package thermal design (Fig. 1). The problem consists of minimizing the thermal resistance between a stream of coolant (U_0, T_0) and a certain volume in space ($L \times H \times W$) in which heat is being generated at the rate q. The overall thermal resistance is $q/(T_{max}-T_0)$, where T_{max} is the highest temperature (the hot-spot temperature) that occurs at a certain point in the heat generating volume.

For the coolant to have access to as many spots as possible in the volume $L \times H \times W$, the heat transfer rate q is generated by (or distributed over) a certain number of parallel plates (n), which form ($n-1$) channels. The coolant flows through the channels, as well as *around* the entire stack of frontal area $H \times W$. The parallel plates are not necessarily equidistant.

The most common application of the thermal design problem described above is in the cooling of a stack of parallel printed-circuit boards. In this case, a reasonable approximation is that the heat generation rate q is distributed uniformly over the $2n$ surfaces, or that the volume averaged heat flux is uniform, $q'' = q/2nLW$. When the stack is held between two larger plates aligned with the $L \times H$ plane and spaced a distance W apart, the flow is essentially two-dimensional.

Another application of this heat removal technique is in the cooling of electronic components fitted over the top with parallel plate fins and bathed by a free stream [1–3]. In Fig. 1, the top of the electronic component would be represented by the base area $L \times H$, which generates the heat transfer rate q. When each plate is thick and conductive enough to function as a "short fin" in the W direction, the plate temperature is mainly a function of the longitudinal position x. The flow can once again be modeled as two-dimensional, especially if the crests of the parallel plate fins are fitted with a shroud of area $L \times H$, whose function is to prevent the loss (or by-pass) of free-stream coolant over the top of the stack.

The geometric optimization of a stack of parallel heat-generating plates has been considered before, in circumstances that differ from the free-stream cooling arrangement of Fig. 1. Most of the published work is about vertical stacks cooled by natural convection [4–6]. In all the natural convection studies, it has been assumed that the plates are positioned equidistantly in the stack, so that the problem was reduced to finding the optimal plate–plate spacing, or the number of plates that should be incorporated in the stack.

In forced convection, there have been numerous numerical studies that dealt with a single plate–plate channel with specified flow through the channel inlet (see the reviews of Incropera [7] and Peterson and Ortega [8]). The plate surfaces were either smooth (flush mounted heat sources) or ribbed (protruding heat sources), as in the studies done by Schmidt and Patankar [9] and Davalath and Bayazitoglu [10]. When the flowrate through the channel was specified there was no optimal plate–plate spacing; instead, the focus was on the effect of the heat source geometry on the temperature distribution in the channel.

An optimal plate–plate spacing for forced convection cooling was derived analytically [11] by minimizing the hot-spot temperature in a two-dimensional stack of swept length L and width H, held between two adiabatic boundaries spaced a distance H apart. The plates were positioned equidistantly in the stack and it was assumed that the pressure differ-

‡Author to whom correspondence should be addressed.

NOMENCLATURE

c_P	fluid specific heat at constant pressure
$C_{1,2}$	constants [equation (22)]
$d_{1,2,\ldots}$	spacings (Figs. 2 and 5)
H	stack width, Fig. 1
k	fluid thermal conductivity
k_s	solid thermal conductivity
k_x	longitudinal thermal conductivity
k_y	transversal thermal conductivity
K_x	longitudinal permeability
L	stack length (Fig. 1)
n	number of plates
P	pressure
Pe_L	Peclet number, U_0L/α
Pr	Prandtl number, ν/α
q	heat transfer rate released by stack
q'	heat transfer rate per unit length, q/W
q''	heat flux, $q'/2nLW$
q'''	volumetric heat generation rate, q'/HL
Re_L	Reynolds number, U_0L/ν
S	flow exit area
T	temperature
T_0	free-stream temperature
T_{max}	maximum (hot-spot) temperature of the stack
u, v	velocity components (Fig. 1)
U	average velocity in parallel-plate channel
U_0	free-stream velocity
W	plate width (Fig. 1)
x, y	Cartesian coordinates (Fig. 1)
x_w, x_e	entrance and exit of the computational domain (Fig. 1)
y_n	width of the computational domain (Fig. 1).

Greek symbols

α	fluid thermal diffusivity
θ	dimensionless temperature [equation (6)]
θ_{hot}	dimensionless hot-spot temperature [equation (11)]
$\theta_{i,max}$	dimensionless maximum temperature on surface i (e.g. Fig. 2)
μ	viscosity
ν	kinematic viscosity
ρ	fluid density
σ_n	normal stress
ϕ	porosity, $d/(d+t)$
Φ	displaced fraction of the free stream (Fig. 7).

Superscript

$(\tilde{})$	dimensionless variables [equations (5, 6)].

Subscripts

$(\,)_{min}$	minimum
$(\,)_{opt}$	optimal.

ence between the inlet plane and the outlet plane of the stack is fixed. Subsequent studies addressed more realistic geometric features such as plates with finite thickness [12], turbulent flow [13], plates cooled individually in parallel-plate channels [14], plates with discrete flush-mounted and protruding heat sources [15] and plate fins with variable thickness and height [16].

On the backdrop provided by the work reviewed above, the free-stream arrangement proposed in Fig. 1 is a step toward a more realistic and general model for the cooling process that occurs in an actual design. In Fig. 1, the free stream is specified; however, the flowrates through the individual channels vary as the designer changes the number of the plates and their relative positions.

Focusing now on the task of optimizing the cooling mechanism in the $L \times H \times W$ space of Fig. 1, we note that the number of degrees of freedom can be quite large (e.g. plate–plate spacings, number of plates), even when the number of plates is small. For this reason, it is important that we conduct the optimization work in a structured manner, so that we can develop the clearest and most general design conclusions without having to make the kind of assumptions that tend to limit the applicability of the results. The structure of our optimization work is represented by three key questions, which are addressed sequentially in the body of the paper:

(a) Is there an optimal way of spacing the plates relative to each other in the given volume?
(b) Is there an optimal number of plates that should be used (installed) in the given volume?
(c) Is it possible to correlate all the individual optimization conclusions into simple (compact) formulas that have wide applicability?

2. MATHEMATICAL FORMULATION AND NUMERICAL METHOD

To optimize the stack geometry in a wide range of flow conditions, we had to develop an efficient way of examining the effect that a change in the stack geometry has on the hot-spot temperature registered inside the stack. We made a very large number of geometry modifications until we arrived at the designs in which the respective hot-spot temperatures are the smallest that they can be. We accomplished this by simulating numerically the flow and temperature fields

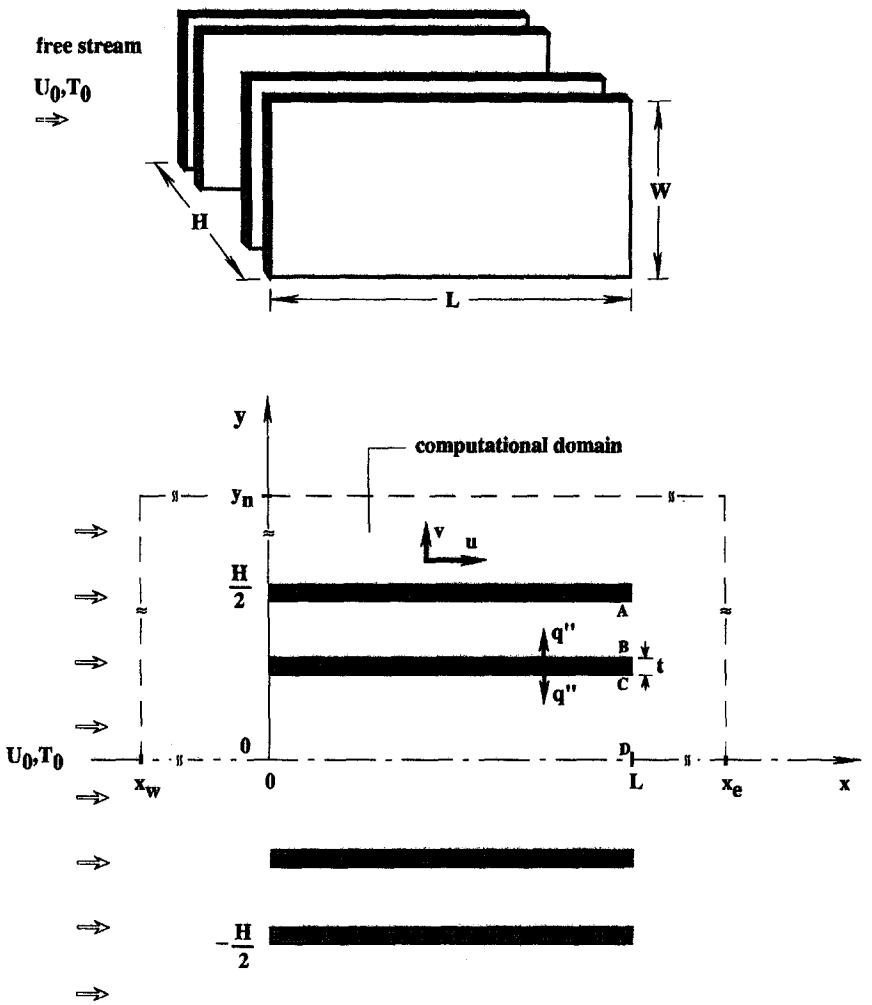

Fig. 1. Stack of nonequidistant plates cooled by a free stream (top) and two-dimensional model and computational domain (bottom).

in the two-dimensional domain shown in the lower part of Fig. 1. For the numerical work, we chose a stack with square cross-section, $H = L$, because the effect of H/L on the optimized geometry can be deduced subsequently, as shown in Section 4. The plate thickness was fixed at $t = L/20$ after a review of the dimensions used in actual designs (e.g. refs. [17, 18]). The Prandtl number effect on the optimal design can also be deduced theoretically (Section 4); therefore, it was set at $Pr = 0.72$ in all the numerical simulations.

The flow was modeled as laminar and incompressible and the fluid was assumed Newtonian with constant properties. Mixed convection effects are assumed negligible. The total rate of heat generation per unit of stack width W was fixed, $q' = q/W$, and distributed uniformly over $2n$ surfaces, $q'' = q'/2nL$ = constant. The dimensionless equations that govern the conservation of mass, momentum and energy in the x–y domain of Fig. 1 are:

$$\frac{\partial \tilde{u}}{\partial \tilde{x}} + \frac{\partial \tilde{v}}{\partial \tilde{y}} = 0 \tag{1}$$

$$\tilde{u}\frac{\partial \tilde{u}}{\partial \tilde{x}} + \tilde{v}\frac{\partial \tilde{u}}{\partial \tilde{y}} = -\frac{\partial \tilde{P}}{\partial \tilde{x}} + \frac{1}{Re_L}\nabla^2 \tilde{u} \tag{2}$$

$$\tilde{u}\frac{\partial \tilde{v}}{\partial \tilde{x}} + \tilde{v}\frac{\partial \tilde{v}}{\partial \tilde{y}} = -\frac{\partial \tilde{P}}{\partial \tilde{y}} + \frac{1}{Re_L}\nabla^2 \tilde{v} \tag{3}$$

$$\tilde{u}\frac{\partial \tilde{\theta}}{\partial \tilde{x}} + \tilde{v}\frac{\partial \tilde{\theta}}{\partial \tilde{y}} = \frac{1}{Pe_L}\nabla^2 \theta, \tag{4}$$

where $\nabla^2 = \partial^2/\partial \tilde{x}^2 + \partial^2/\partial \tilde{y}^2$. The dimensionless variables indicated with ˜ are defined as follows:

$$\tilde{x}, \tilde{y} = \frac{(x, y)}{L}, \quad (\tilde{u}, \tilde{v}) = \frac{(u, v)}{U_0} \tag{5}$$

$$\tilde{P} = \frac{P}{\rho U_0^2}, \quad \theta = \frac{T - T_0}{q'/k} \tag{6}$$

Table 1. Tests for determining the outer boundaries of the computational domain ($Re_L = 200$, $n = 4$, equidistant plates). The exit planes AB and CD are marked on the lower drawing of Fig. 1

Geometry		Integral normal stress		Average heat flux					
				AB			CD		
x_e	x_w	AB	CD	Diffusion	Convection	Total	Diffusion	Convection	Total
−0.8	2.0	0.036342	0.018929	0.015337	1.89039	1.90573	0.014658	1.85173	1.86639
−1.0	2.0	0.033396	0.017223	0.015455	1.88809	1.90352	0.014730	1.84988	1.86461
−1.2	2.0	0.031398	0.016102	0.015526	1.88560	1.90113	0.014764	1.84861	1.86337
−1.4	2.0	0.029995	0.015351	0.015565	1.88328	1.89885	0.014778	1.84773	1.86251
−1.8	2.0	0.028391	0.014464	0.015612	1.88008	1.89570	0.014789	1.84649	1.86128
−2.0	3.0	0.029958	0.015238	0.015194	1.87933	1.89453	0.014274	1.84639	1.86066
−2.0	3.5	0.030723	0.015627	0.014844	1.87974	1.89459	0.013862	1.84696	1.86082

$$Re_L = \frac{U_0 L}{\nu}, \quad Pe_L = \frac{U_0 L}{\alpha} = Re_L Pr. \tag{7}$$

The physical (dimensional) variables are defined in the Nomenclature. The boundary conditions imposed around the computational domain are:

$$\tilde{u} = 1, \tilde{v} = 0, \theta = 0 \quad \text{at} \quad \tilde{x} = \tilde{x}_w \text{ and } \tilde{y} \in (0, \tilde{y}_n) \tag{8}$$

$$\frac{\partial \tilde{u}}{\partial \tilde{y}} = 0, \tilde{v} = 0, \quad \frac{\partial \theta}{\partial \tilde{y}} = 0 \quad \text{at} \quad \tilde{x} \in (\tilde{x}_w, \tilde{x}_e) \text{ and } \tilde{y} = 0, \tilde{y}_n \tag{9}$$

$$\int_{\tilde{S}} \tilde{\sigma}_n \, d\tilde{S} = 0, \quad \frac{\partial \theta}{\partial \tilde{x}} = 0 \quad \text{at} \quad \tilde{x} = \tilde{x}_e \text{ and } \tilde{y} \in (0, \tilde{y}_n), \tag{10}$$

where $\tilde{S}$ is the plane of the exit and $\tilde{\sigma}_n$ is the normal stress, $\tilde{\sigma}_n = \sigma_n / \rho U_0^2$. All the plate surfaces were modeled as no-slip, impermeable and with uniform heat flux q'' pointing into the fluid.

It should be noted that the numerical task of simulating the flow and temperature fields in a stack cooled by a free stream (the present problem) is considerably more challenging and time consuming than when the stack is itself sandwiched between two longer parallel plates (e.g. refs. [6, 11]). In the latter, there is no coolant by-pass around the stack and, when the plates are equidistant, it is sufficient to perform calculations only for one plate–plate channel.

The calculations were performed using the finite element software package FIDAP [19]. The ability of this package to handle flows of the same class as the present ones was demonstrated based on benchmark problems [19, 20]. The extent of the computational domain $(\tilde{x}_w, \tilde{x}_e, \tilde{y}_n)$ was chosen such that the flow behaves as a free stream (i.e. is not affected by the stack) in regions situated sufficiently far from the stack. As tests, we used (1) the normal stress integral over the exit plane $[\tilde{x} = 1, y \in (0, 1/2)]$, (2) the $\tilde{v}$ component at the outer edge of the domain $(\tilde{y} = \tilde{y}_n)$, so that $\tilde{v}$ was less than 1% and (3) the heat fluxes through the exit plane $(\tilde{x} = 1)$ of the plate–plate channels. Some of these tests are repeated in Table 1 for $Re_L = 200$ and $n = 4$. The values determined in this manner and used in all the simulations are $\tilde{x}_e = 3$, $\tilde{x}_w = -2$ and $\tilde{y}_n = 2$.

The symmetry about $\tilde{y} = 0$ allowed us to perform the calculations in only half of the field, namely $0 < \tilde{y} < \tilde{y}_n$. For stacks with four plates, grid independent solutions were obtained by using 4852 quadratic, isoparametric, rectangular, nine-node elements. The number of elements was increased to 5138 as the number of plates increased to $n = 9$. A discontinuous pressure model with a penalty factor of 10^{-6} was used. The operator residual and the velocity residual were set at 10^{-3}. Successive substitutions with an attenuation factor of 0.4 and quasi-Newton (Broyden update, with reformation of the Jacobian after every five iterations) algorithms were used. For the basic runs, which lasted about 1200 s each, we used the CRAY Y-MP at the North Carolina Supercomputing Center, with local IRIS workstations as front end for pre- and post-processing. Approximately 15 c.p.u. CRAY hours were necessary for completing this work.

3. HOW TO SPACE THE PLATES RELATIVE TO ONE ANOTHER

The first design question we addressed was how to position the plates relative to one another in the stack, for example, equidistantly, or in some optimal uneven fashion as in the lower part of Fig. 1. The number of plates in the stack, n, is fixed. This question is particularly important in a design with few plates, say $n = 4$, because the two outer plates account for half of the total heat transfer area. From the outset, we expect the cooling of an outer plate to differ from the cooling of a plate sandwiched by other plates.

For this reason and for the sake of illustrating the optimization method in the simplest terms possible, we present in detail the optimization of the relative spacings in a stack with four plates (Figs. 2–4). As shown at the top of Fig. 2, the design has only 1 degree of freedom, represented by the half-spacing d_1, or the position of the internal plate. The sum of the two spacings is fixed, $d_1 + d_2 = (L/2) - 2t$.

For each flow (e.g. $Re_L = 200$ in Fig. 2), we cal-

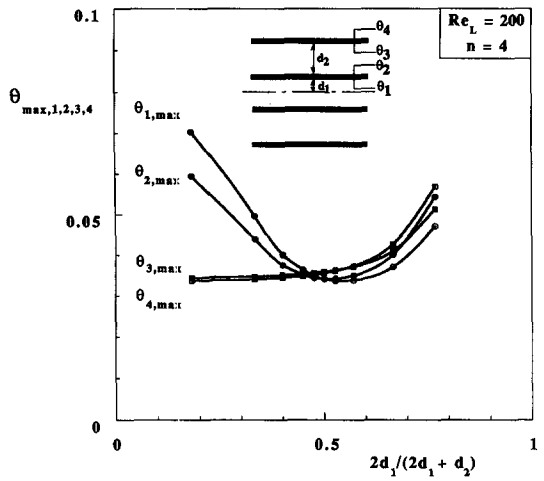

Fig. 2. The effect of the position of the inner plates on the maximum temperatures of the plate surfaces ($n = 4$, $Re_L = 200$).

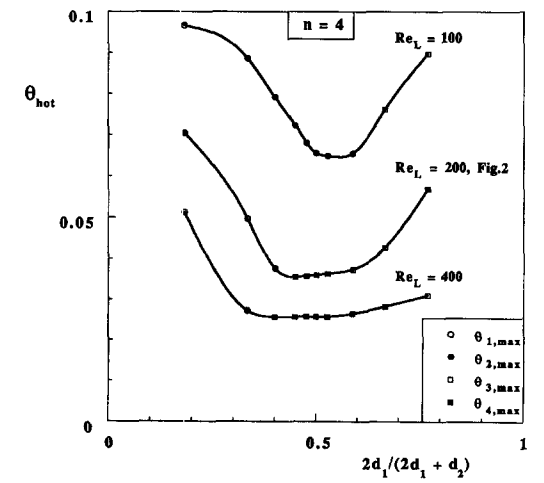

Fig. 3. The effect of the position of the inner plates on the hot-spot temperature of the entire stack ($n = 4$).

culated the temperature distributions over all the surfaces. There are four such distributions, θ_1, θ_2, θ_3 and θ_4. On each surface, we identified the location and value of the maximum temperature. The four temperature maxima are plotted in dimensionless terms ($\theta_{1,max}, \ldots, \theta_{4,max}$) in the lower part of Fig. 2. These temperature maxima occur close to the trailing edge of each surface (e.g. Fig. 4).

The abscissa of Fig. 2 accounts for changes in the relative position of the inner plate: it is very clear that this position can be selected such that the peak temperature of the entire stack is minimized. Of interest, then, is the minimization of the largest of the four temperature maxima, or the dimensionless hot-spot temperature,

$$\theta_{hot} = \max(\theta_{1,max}, \theta_{2,max}, \theta_{3,max}, \theta_{4,max}). \quad (11)$$

This second step of the optimization method is presented in Fig. 3. The symbols that are superimposed on the curve $Re_L = 200$ indicate which of the four temperature maxima is the largest, i.e. the surface on which the hot spot is located. The hot spot jumps from one surface to another as the position of the inner plate changes.

Next to the $Re_L = 200$ data derived from Fig. 2, in Fig. 3 we plotted the corresponding results developed for $Re_L = 100$ and $Re_L = 400$. The effect of the inner plate position is clear: the hot-spot temperature θ_{hot} is always the lowest when $2d_1/(2d_1+d_2)$ is close to 0.5, i.e. when the plates are positioned equidistantly. The minimum exhibited by θ_{hot} is sufficiently flat in the vicinity of $2d_1/(2d_1+d_2) \cong 0.5$ to recommend with confidence that the optimal design for $n = 4$ and $Re_L = 100$–400 is the one in which the plates are positioned equidistantly. The θ_{hot} minimum becomes flatter as Re_L increases: this means that the equidistant positioning of the boards becomes less critical as the Reynolds number increases.

One interesting aspect of the flows and geometries summarized in Fig. 3 is that the position of the hot spot changes not only with the geometry $[2d_1/(2d_1+d_2)]$ but also with the flow (Re_L). When Re_L is small, the hot spot is located always inside the stack, i.e. on one of the surfaces that do not face the free stream. When Re_L is equal to 200 or greater and when the inner plate spacing is close to optimal, the hot spot occurs near the trailing edge of the external surface bathed by the free stream ($\theta_{hot} = \theta_{4,max}$). This feature is unexpected and is due to the development of a roll on top of the external surface as Re_L increases. The streamline patterns of Fig. 4 illustrate this effect: the actual position of the hot-spot temperature is indicated with a small circle. In Fig. 4, the streamfunction is defined by $\tilde{u} = \partial\tilde{\psi}/\partial\tilde{y}$ and $\tilde{v} = -\partial\tilde{\psi}/\partial\tilde{x}$.

The optimization procedure of Figs. 2 and 3 was repeated for a stack with six plates. As shown in Fig. 5, when $n = 6$ the design has 2 degrees of freedom associated with the positions of the two inner plates [or d_1 and d_2, with $d_1+d_2+d_3 = (L/2)-3t = \text{constant}$]. The numerical work was considerably more extensive than for the stack with four plates; therefore, in Fig. 5, we show the effect of only one of the degrees of freedom on the value and position of the hot-spot temperature. In plotting Fig. 5, we fixed the innermost half space at $d_1/L = 0.07$, while varying the position of the next internal plate (with surface temperatures T_3 and T_4). The lowest hot-spot temperature occurs in the vicinity of the design represented by $d_2/(d_2+d_3) = 0.5$, which means that the optimal position of the movable plate (θ_3, θ_4) is halfway between the innermost plate (θ_1, θ_2) and the external plate (θ_5, θ_6). In this optimal case, the hot spot occurs near the trailing edge of the third surface, $\theta_{hot} = \theta_{3,max}$.

By repeating the plot of Fig. 5 for other combinations of d_1/L and Re_L, we were able to strengthen the conclusion that in the Re_L range 100–400 the low-

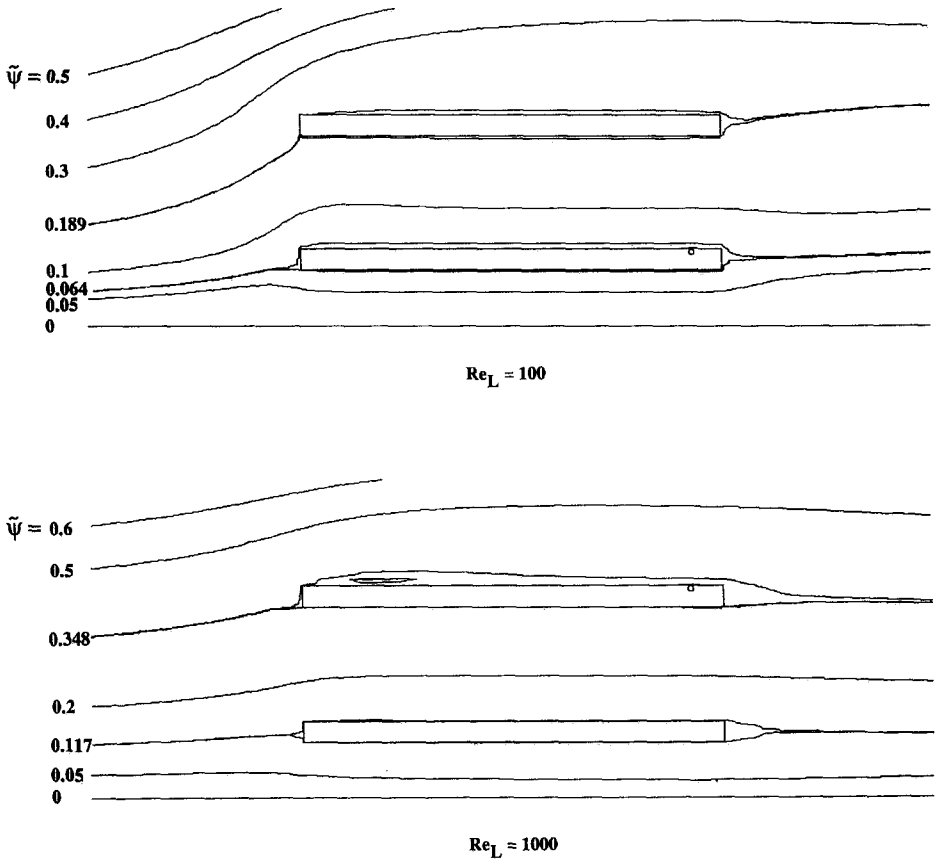

Fig. 4. The effect of the Reynolds number on the position of the hot spot ($n = 4$, equidistant plates).

est hot-spot temperature is attained when the six plates are positioned equidistantly ($2d_1 = d_2 = d_3$). The effect shown in Fig. 4 is encountered again: as Re_L increases, the hot spot migrates from one of the internal surfaces to the trailing section of the external surface ($\theta_{hot} = \theta_{6,max}$).

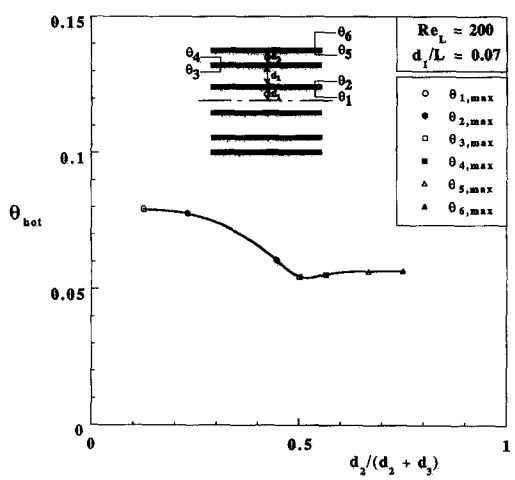

Fig. 5. Stack with six plates: the response of the hot-spot temperature to changes in the position of one of the internal plates ($n = 6$, $Re_L = 200$).

If we compare the $Re_L = 200$ results for four plates (Fig. 3) with the corresponding results for six plates (Fig. 5), we see that the geometry-induced changes in the hot-spot temperature are smaller when n is greater. This means that the fine-tuning of the position of each plate relative to its two neighbors loses its importance as n increases. Since the best designs for $n = 4$ and $n = 6$ are the ones in which the plates are spaced equidistantly, it is safe to generalize and to recommend the equidistant spacing as an optimal design feature for stacks with more than six plates.

4. OPTIMAL NUMBER OF EQUIDISTANT BOARDS

The second design aspect we investigated was whether the number of boards installed in the stack can be selected optimally, so that the hot-spot temperature is minimized. We assumed that the n boards are positioned equidistantly in the stack, in accordance with the conclusions reached in the preceding section. The total heat transfer rate removed from the stack of cross-sectional area $L \times H$ was equal to q' [cf. equation (6)], i.e. independent of the number of boards.

For each number of boards (n) and set of flow conditions (Re_L), we determined the hot-spot tem-

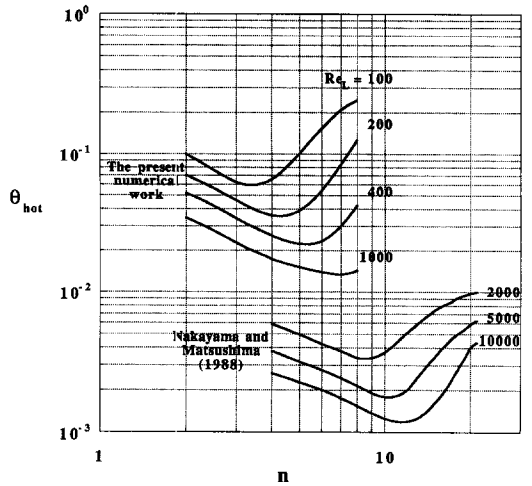

Fig. 6. The effect of the number of equidistant plates on the hot-spot temperature.

perature θ_{hot}. The results are presented in Fig. 6, for the range $2 \leqslant n \leqslant 8$ and $100 \leqslant Re_L \leqslant 1000$. It is clear that there exists an optimal number of boards and that knowing this number accurately makes a difference in the effort to maximize the overall thermal conductance (the inverse of θ_{hot}). The $n_{opt}(Re_L)$ values identified with the help of Fig. 6 are recorded in Table 2.

In order to correlate our n_{opt} results and extend their validity outside the (n, Re_L) range of Fig. 6, we reexamined the conclusions reached in Bejan and Sciubba's [11] study of a stack with parallel equidistant plates and imposed pressure difference ΔP between $x = 0$ and $x = L$. In that study, the plate–plate channel flows were identical, because the stack was cooled in the two-dimensional channel formed between two adiabatic plates with the distance H in-between (i.e. no free stream around the stack). It was assumed further that the plate thickness is negligible, and that the plate–plate spacing d is small when compared with H, or that the number of plates is large, $n = H/d \gg 1$. The analysis produced the following optimal spacing for a stack with uniform flux on both sides of each plate:

$$\frac{d_{opt}}{L} \cong 3.2\left(\frac{\Delta P \cdot L^2}{\mu\alpha}\right)^{-1/4} \quad (Pr \geqslant 0.7). \tag{12}$$

It can be shown by generalizing the analysis of ref. [11] that equation (12) holds even when the plate thickness is not negligible when compared with the plate–plate spacing [12].

In the cooling arrangement of Fig. 1, the free-stream velocity U_0 is specified, not the pressure drop across the stack. In the stack of Fig. 1, there are several pressure drops, one for each plate–plate channel. It is reasonable to expect that, as the number of plates increases, the order of magnitude of the pressure drop is the stagnation pressure scale

$$\Delta P \sim \frac{1}{2}\rho U_0^2 \tag{13}$$

and that this scale is the same for all the channels. In accordance with the model of ref. [11], we assume that $n_{opt} \gg 1$, where

$$n_{opt} \cong \frac{H}{d_{opt} + t} \gg 1. \tag{14}$$

By eliminating ΔP and d_{opt} between equations (12)–(14), we obtain an estimate for the spacing in terms of the free-stream conditions ($Re_L = U_0 L/\nu$),

$$\frac{d_{opt}}{L} \cong \frac{3.8}{Pr^{1/4} Re_L^{1/2}} \tag{12'}$$

and, for the optimal number of boards,

$$n_{opt} \cong \frac{0.26\dfrac{H}{L} Pr^{1/4} Re_L^{1/2}}{1 + 0.26\dfrac{t}{L} Pr^{1/4} Re_L^{1/2}} \quad (Pr \geqslant 0.7, n \gg 1). \tag{15}$$

The n_{opt} values calculated based on equation (15) have been added to Table 2. The agreement between the rounded (integer) values of these order-of-magnitude estimates and the numerical data furnished by Fig. 6 is good, even though the number of boards is small, i.e. outside the range of equation (15). The relative agreement improves as Re_L increases. This

Table 2. Summary of results for the optimal number of equidistant plates

	Re_L								
n_{opt}	100	200	400	1000	2000	4000	5000	6000	10 000
The present numerical work (Fig. 6)	3	4	5	7					
The theoretical correlation [equation (15)]	2.1	2.9	3.9	5.5	7.2‡	12.1†	9.6‡	14.2†	11.5‡
From Fig. 6 of Nakayama *et al.* [2]					8		10		12
From the experiments of Matsushima *et al.* [3]						12–13		15–17	

†Calculated using $t/L = 1/60$ in equation (15).
‡Calculated using $t/L = 0.0455$ in equation (15).

Table 3. Summary of results for minimum hot-spot excess temperature

$\theta_{\text{hot,min}} \frac{H}{L} Pr^{1/2} Re_L$ [equation (17)]	Re_L								
	100	200	400	1000	2000	4000	5000	6000	10 000
The present numerical work (Fig. 6)	5.1	5.9	7.1	11.3					
From Fig. 6 of Nakayama *et al.* [2]					5.7		7.6		10.1
From the experiments of Matsushima *et al.* [3]						8.8		9.9	

trend is supported further by the independent data described in the next section.

In conclusion, in the small Re_L range 100–1000 we may use equation (15) provided we add 1 to the calculated n_{opt} value. An additional advantage of equation (15) is that it shows analytically the effects of the stack aspect ratio (H/L), the board thickness (t/L) and the Prandtl number. Recall that the present numerical results were obtained by setting $H/L = 1$, $t/L = 1/20$ and $Pr = 0.72$.

The analysis of the two-dimensional stack held in a parallel-plate duct [11] produced also an estimate for the scale of the maximum thermal conductance that corresponds to the optimal equidistant spacing (12), namely

$$\left(\frac{q'}{T_{\max} - T_0}\right)_{\max} \cong 0.4 c_p H \left(\frac{\rho \Delta P}{Pr}\right)^{1/2}. \quad (16)$$

This estimate holds for $Pr \gtrsim 0.7$, $n \gg 1$ and $t \ll d$. If we eliminate ΔP using the pressure scale (13) and if we use the θ definition (6), we can rearrange equation (16) as a theoretical scale of the minimum dimensionless hot-spot temperature,

$$\theta_{\text{hot,min}} \cong 3.5 \frac{L}{H} Pr^{-1/2} Re_L^{-1}$$

$$(Pr \gtrsim 0.7, n \gg 1, t \ll d). \quad (17)$$

This scale is tested in Table 3 by using the minimum θ_{hot} value identified in Fig. 6 for $H/L = 1$ and $Pr = 0.72$. Table 3 shows that equation (17) is correct in an order of magnitude sense and that it accounts well for large changes in Re_L. The same table shows that the best correlation of type (17) is obtained if the 3.5 factor is replaced with approximately 7.6. We will improve the correlation (17) in the next section, after we review a series of experimental results.

Before we close this presentation of the numerical optimization of stacks with equidistant boards, we find it interesting to review the features of the flow through and around the stack (Fig. 4). The stack displaces a significant fraction of the free stream that would be flowing through the space $L \times H$ when the stack is absent. The volumetric flowrate through the entrance plane

$$\left(x = 0, -\frac{H}{2} \leqslant y \leqslant \frac{H}{2}\right)$$

when the stack is absent is $U_0 H$. The flowrate displaced by the stack is

$$U_0 H - \int_{-H/2}^{H/2} (u)_{x=0} \mathrm{d}y. \quad (18)$$

A relative measure of the displaced (lost) flowrate is the ratio (displaced fraction)/(flowrate when the stack is absent):

$$\Phi = 1 - \frac{1}{U_0 H} \int_{-H/2}^{H/2} (u)_{x=0} \mathrm{d}y. \quad (19)$$

This ratio has been calculated for all the flows discussed in this section and plotted in Fig. 7. The displaced fraction Φ approaches 1 as n increases and Re_L decreases. In other words, as the number of plates increases and, if their thickness remains fixed, the total cross-sectional area of the channels decreases to such an extent that most of the original flowrate $U_0 H$ flows around the stack. By combining Fig. 7 with the n_{opt} values reported in Table 2, we also note that, in stacks with optimal numbers of plates, the displaced flow fraction Φ increases as Re_L increases.

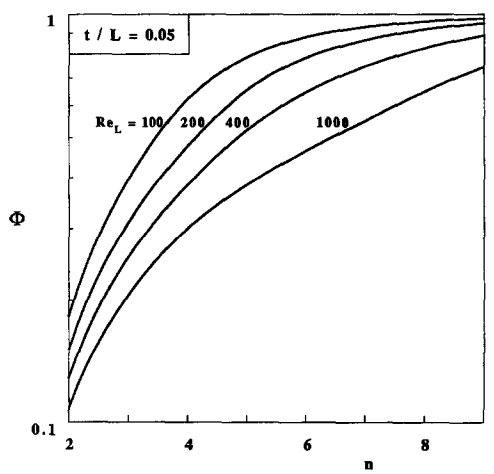

Fig. 7. The fraction of the original free stream that is displaced by the stack and flows around the stack (equidistant plates).

5. COMPARISON WITH EXPERIMENTAL RESULTS, AND EXTENSION TO HIGHER REYNOLDS NUMBERS

Nakayama *et al.* [2] performed experiments with square packages ($L = H = 22$ mm) fitted with seven parallel and equidistant plate fins ($W = 12$ mm, $t = 1$ mm) cooled in a free stream of air. The Reynolds number Re_L varied in the range 10^3–10^4. The base area $L \times H$ was heated uniformly. The heat transfer and temperature measurements were reduced using an analysis based on a numerical model described earlier by Ashiwake *et al.* [21]. In the model, the plate surfaces were assumed isothermal and the channel flow was of the entrance (developing) type. Nakayama *et al.* [2] used this model to reproduce their measurements and to anticipate, on a case-by-case basis, what would happen if the number of plate fins changes.

We have translated their results into the present notation and projected them on Fig. 6. This addition is justified because, in the experiments, the ratio $t/L = 0.0455$ was nearly the same as in the present numerical work ($t/L = 0.05$). The fin efficiency of the plates used in the experiment was greater than 0.95. This means that the experimental plates were nearly isothermal in the W direction, which is in agreement with the assumption that led to the two-dimensional model employed in the numerical work (Fig. 1, bottom).

Figure 6 shows that the results of Nakayama *et al.* mesh very nicely with the present numerical results. The optimal number of plates for minimum θ_{hot} according to Nakayama *et al.* has been added to Table 2, along with the corresponding calculations based on the theoretical correlation (15). This comparison shows that, indeed, equation (15) becomes more accurate as n increases. Note that the rounded (integer) n_{opt} value predicted by equation (15) matches the value recorded by Nakayama *et al.* when Re_L exceeds 5000.

To Table 3, we have added the minimum θ_{hot} values read off the curves from Nakayama *et al.* in Fig. 6. We estimate a possible error of the order of 5% in our technique of deducing θ_{hot} values from Nakayama *et al.* [2], because the original source of these data was a graph with relatively thick curves and without mesh. Table 3 shows that these high-Re_L data support very well the trend anticipated theoretically in equation (17).

The accuracy of the numerical model employed by Nakayama *et al.* [2] was tested based on laboratory measurements by Matsushima *et al.* [3]. These authors experimented with finned packages mounted in a parallel plate channel with a vertical spacing of 28 mm, which was greater than the fin height $W = 18$ mm. The other dimensions were $L = H = 60$ mm and $t = 1$ mm. The fins were equidistant and their number was varied from 8 to 17. The measurements showed a discrepancy of less than 11% between the measured overall thermal conductance between the package and the air stream and the thermal conductance anticipated based on the numerical model.

In Tables 2 and 3 we have added the n_{opt} and $\theta_{hot,min}$ values found experimentally by Matsushima *et al.* [3] using the free-stream air velocities 1 and 1.5 m s^{-1}, which, at room temperature, correspond to $Re_L = 4000$ and 6000. The experimental values agree very well with the two sets discussed previously, even though in the experiments of Matsushima *et al.* the t/L ratio was approximately half of the previous ratio. The theoretical correlations (15) and (17) are further strengthened by these experimental results. Once again, the correlation (17) works best if the 3.5 factor on the right side is replaced by approximately 7.6.

The accuracy of the correlation (17) can be improved by accounting for the effect of the board thickness. If we consider the fact that the thickness t is not always negligible with respect to the board to board spacing d, we can repeat (and generalize) the order of magnitude analysis of Bejan and Sciubba [11] and obtain [in place of equation (16)]:

$$\left(\frac{q'}{T_{max}-T_0}\right)_{max} \cong \frac{0.4c_P H}{1+t/d_{opt}}\left(\frac{\rho\Delta P}{Pr}\right)^{1/2}. \quad (20)$$

The difference between this and equation (16) is the $(1+t/d_{opt})$ group in the denominator, in which d_{opt} is independent of the board thickness even when t is not negligible [cf. equation (12)]. Next, we substitute the ΔP scale (13) in equation (20) and obtain the following estimate in place of equation (17):

$$\theta_{hot,min} = C_1 \frac{L}{H}\frac{1+C_2(t/L)Re_L^{1/2}}{Pr^{1/2}Re_L} \quad (Pr \gtrsim 0.7, n \gg 1), \quad (21)$$

in which C_1 and C_2 are two dimensionless constants of order 1. Equation (21) was fitted by least squares to the $\theta_{hot,min}$ data produced in this study and in Matsushima *et al.* [3] (Table 3) and the constants that represent the best fit are

$$C_1 = 1.85 \quad \text{and} \quad C_2 = 3.27. \quad (22)$$

The standard deviation between equations (21, 22) and the mentioned data is 0.4%. The $\theta_{hot,min}$ data of Nakayama *et al.* [2] are about three times smaller than the values calculated based on the generalized correlation (21, 22). Note finally that equation (21) holds in the range of *finite* Re_L values covered by this study (Tables 2 and 3). It does not mean that $\theta_{hot,min} \to \infty$ if $Re_L \to 0$.

The scaling theory of ref. [11] showed that the class of optimization rules to which the present results [equations (12, 15, 21, 22)] belong corresponds to flows in which the channel length L is of the same order as the thermal entrance length of each channel. This means that, when the coolant has a Prandtl number of order 1 (e.g. air), the velocity boundary layers meet at the trailing edge of each parallel-plate channel. The laminar flow prevails as long as the order of Re_L is less than 2×10^5, which is equivalent to a channel Reynolds number $U(2d_{opt})/\nu$ less than 2000 [22].

Table 4. Results obtained by treating the stack as a porous medium with Darcy flow: $Re_L = 400$; $k_s/k = 0$; $H/L = 1$; $Pr = 0.72$; $t/L = 0.05$; $d/L = 0.0688$. Listed in parentheses are the corresponding values obtained with the model of Section 2 for $n = 9$

Re_L	θ_{hot}	Φ	CPU time (s)	Iterations
100	0.321	0.9751	761	13
	(0.459)	(0.9751)	(1911)	(13)
200	0.306	0.9456	1044	18
	(0.332)	(0.9486)	(2646)	(18)
400	0.114	0.8790	1218	21
	(0.135)	(0.8857)	(2793)	(19)

6. THE STACK WITH MORE PLATES THAN THE OPTIMAL NUMBER, MODELED AS AN ANISOTROPIC POROUS MEDIUM WITH DARCY FLOW

The entrance-region character of the channel flow in the optimal design ($d = d_{opt}$) means that, when the coolant free-stream velocity is less than the specified design value (U_0), most of the channel flow is in the fully developed regime (Hagen–Poiseuille). Such an off-design condition is equivalent to installing more boards than the optimal number in the present stack (Fig. 1, top, with the full U_0 around the stack), or using channels that are narrower than the optimal spacing found in equations (12, 12′), $d < d_{opt}$.

The performance of the stack (its hot-spot temperature) can be determined numerically using the method of Section 2 for any channel spacing, including $d < d_{opt}$. It is important to note that, when $d < d_{opt}$ and the channel flow is of the Hagen–Poiseuille type, the temperature distribution in the volume occupied by the stack can be calculated considerably faster (e.g. Table 4) if the stack volume is treated as a saturated homogeneous anisotropic porous medium with Darcy flow in the x direction. The porous medium model has the added advantage that it accounts (in a volume averaged sense) for the conduction through the board material, longitudinally and transversally. Below, we list only the modifications that the porous medium model brings into the numerical formulation described in Section 2.

The equations and far-field conditions for the flow and heat transfer in the regions situated outside the stack remain unchanged. Inside the $H \times L$ space, the flow is purely longitudinal ($v = 0$), with the velocity

$$u = -\frac{K_x}{\mu}\frac{\partial P}{\partial x}, \tag{23}$$

which is constant from $x = 0$ to $x = L$, but may vary in the y direction. The K_x permeability of a stack with boards spaced equidistantly (spacing = d, board thickness = t) is a known constant (e.g. ref. [23]):

$$K_x = \frac{d^3}{12(t+d)} = \frac{d^2}{12}\phi, \tag{24}$$

where $\phi = d/(d+t)$ is the stack porosity. The u velocity is a volume averaged quantity, which, based on mass conservation, corresponds to the u component immediately outside the stack (in the pure fluid, at $x = 0^-$ and $x = L^+$). The porous medium is impermeable in the transversal direction.

The u velocity inside the porous medium is a function of y because it is driven by the pressure difference between the entrance and exit of an individual channel, $-\partial P/\partial x = [P(0,y) - P(L,y)]/L$. This pressure difference is maximum across the channel positioned along the midplane ($y = 0$) and smaller near the lateral edges ($y = \pm H/2$). In the numerical implementation of the porous medium model, it is assumed that P varies continuously across the entrance and exit planes of the stack ($x = 0, L$).

The temperature distribution inside the $H \times L$ space is governed by the new energy equation:

$$\rho c_P u\frac{\partial T}{\partial x} = k_x\frac{\partial^2 T}{\partial x^2} + k_y\frac{\partial^2 T}{\partial y^2} + q''', \tag{25}$$

which replaces equation (4). Local thermal equilibrium is assumed, so that T represents the local temperature of the solid and adjacent fluid. The total heat generation rate of the stack (q') is distributed uniformly over the stack volume, $q''' = q'/HL$. Given the parallel-plates structure of the porous medium (many plates are assumed), the directional thermal conductivities (k_x, k_y) can be estimated based on the parallel resistance and series resistance models (e.g. ref. [24]):

$$k_x = \phi k + (1-\phi)k_s \tag{26}$$

$$k_y = \frac{kk_s}{(1-\phi)k + \phi k_s}, \tag{27}$$

where k_s is the thermal conductivity of the solid phase (the board material). The temperature T varies continuously across the boundary of the $H \times L$ space.

Finally, when we nondimensionalize the energy equation (25) using the variables defined earlier in equations (5, 6), we find that the dimensionless temperature inside the stack depends on eight variables, $\theta = \theta[\tilde{x}, \tilde{y}, H/L, Pr, Re_L, d/L, t/L \text{ (or } \phi), k_s/k]$. The hot spot occurs at or near the exit from the stack, as will

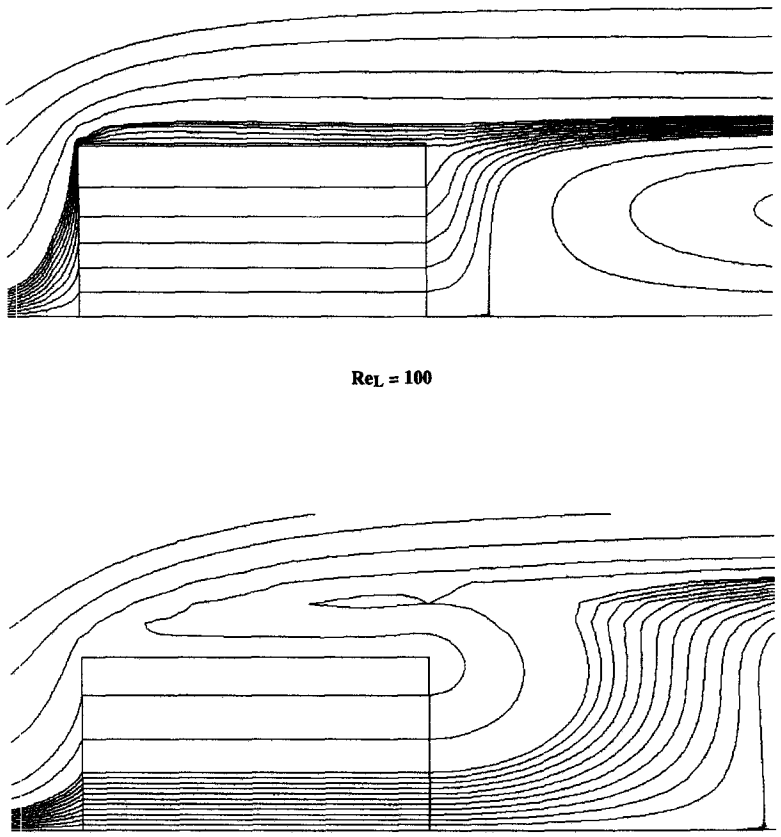

Fig. 8. The flow pattern when the stack is treated as a porous medium ($H/L = 1$, $Pr = 0.72$, $t/L = 0.05$, $d/L = 0.0688$).

be illustrated by the isotherm patterns of Fig. 9. The dimensionless hot-spot temperature depends on a total of six parameters, $\theta_{hot} = \theta_{hot}(H/L, Pr, Re_L, d/L, t/L, k_s/k)$.

The most important questions that can be answered numerically by using the above model are: (a) what is the effect of the conductivity ratio k_s/k on the hot-spot temperature; and (b) how accurate and more efficient is this simpler model relative to the complete model described in Section 2? We investigated these aspects by fixing (as in Sections 2–5) several parameters, namely $H/L = 1$, $Pr = 0.72$ and $t/L = 1/20$.

As a first example, we chose an external flow with $Re_L = 400$, for which Fig. 6 showed that the optimal number of boards is $n_{opt} = 5$. To place the actual channel flow in the Hagen–Poiseuille regime, we chose a larger number of boards, namely $n = 9$. The other geometric parameters that follow from this choice are $d/L = 0.0688$ and $\phi = 0.579$.

The flow pattern calculated for $Re_L = 400$ using the stack porous medium model is shown in the lower part of Fig. 8. The base of the drawing (the lowest streamline) is the plane of symmetry of the stack, $y = 0$. Only the external flow situated in the immediate vicinity of the stack is shown (the computational domain is considerably more extensive, as indicated at the end of Section 2). Figure 8 shows that most of the fluid that flows through the stack prefers the channels that are close to the plane of symmetry. The flow through the stack is more uniform when Re_L is smaller, as shown in the upper drawing of Fig. 8.

The isotherm patterns that correspond to the $Re_L = 400$ flow are presented in Fig. 9. We see that the temperature distribution inside the stack is influenced greatly by the thermal conductivity ratio k_s/k. Furthermore, the position of the hot spot is dictated by k_s/k. When k_s/k is small (Fig. 9, top), the hot spot occurs near the exit from one of the outer (peripheral) parallel-plate channels, because the flow through that channel is relatively weak (Fig. 8, bottom). In the opposite extreme, a large k_s/k ratio means that the stack is cooled in the transversal direction by the fluid that flows around the stack. In this limit, the hot spot occurs near the exit from the channel that coincides with the plane of symmetry. The hot spot migrates

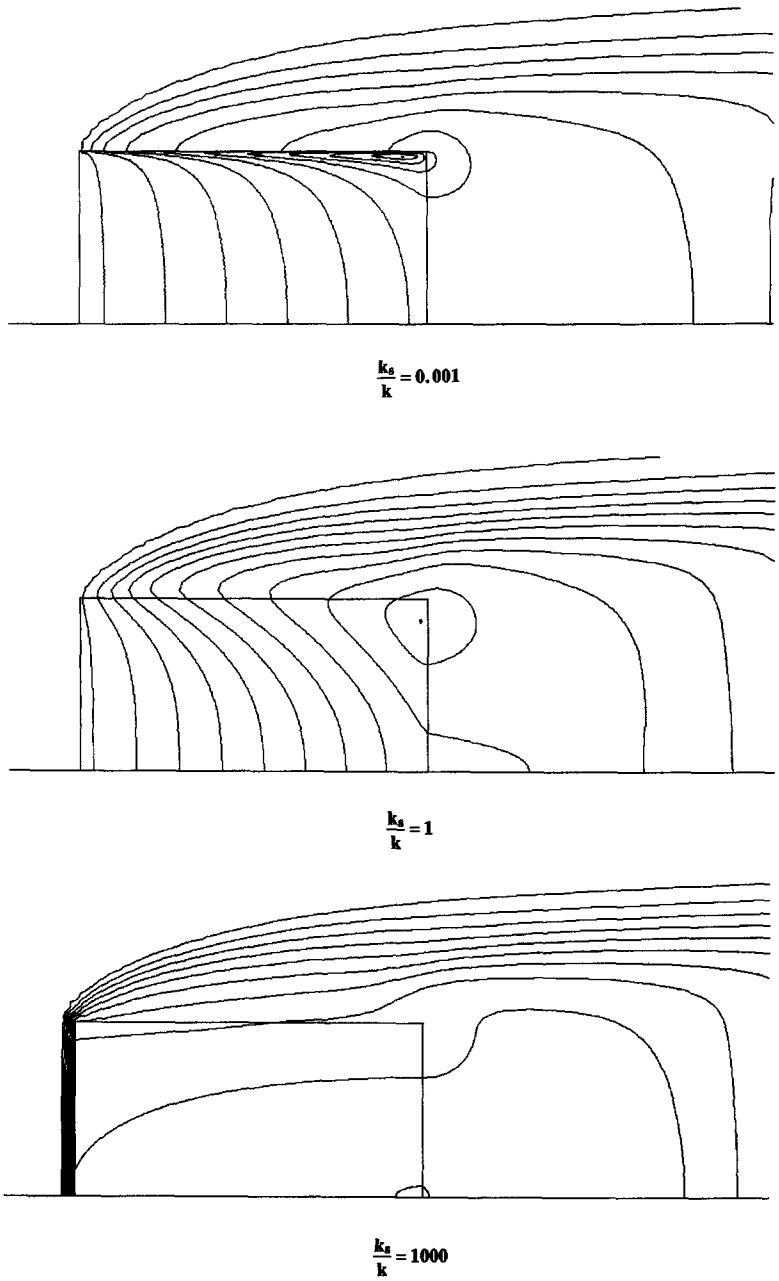

Fig. 9. The temperature distribution that corresponds to the $Re_L = 400$ flow shown in Fig. 8.

from one position to the other when k_s/k is of order 1.

The additional cooling effect due to transversal conduction is even more evident in Fig. 10. The hot-spot excess temperature θ_{hot} decreases to about one-fifth of its original value as k_s/k increases from 0 to 10^4. Figure 10 also summarizes the corresponding conclusions obtained for two additional examples, $Re_L = 100$ and 200. The θ_{hot} value is larger when Re_L is smaller: this trend agrees with what we saw in Fig. 6 by using the model of Section 2.

Finally, in Table 4, we show a comparison between the results obtained with the two models, specifically the porous stack model with $k_s/k = 0$ and the model of Section 2 for a stack with nine plates. The Section 2 model is represented by the values placed in parentheses. The agreement between the two sets of θ_{hot} values is quite good. The fraction of the displaced flow Φ calculated with the porous medium model is virtually the same as the fraction calculated with the model of Section 2. The table shows that the loss in the accuracy with which the porous medium model predicts θ_{hot} is balanced by a gain in computational speed. The porous medium model has the additional advantage that it documents the effect of the thermal conductivity ratio.

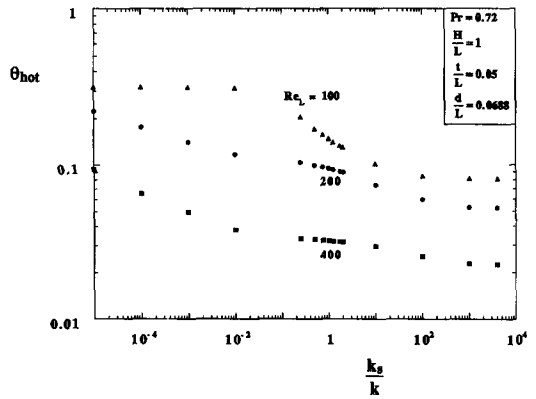

Fig. 10. The hot-spot excess temperature obtained by treating the stack as a porous medium.

7. CONCLUSIONS

In this paper, we addressed the fundamental heat transfer augmentation problem of how to cool a stack of parallel plates immersed in a free stream. We investigated this problem in four distinct phases, with the following key conclusions:

(a) The best way of positioning the plates relative to one another is by spacing them equidistantly. The relative positioning of the plates becomes less critical as the number of plates increases.

(b) When the free stream and the overall dimensions of the stack are specified, there is an optimal number of plates that minimizes the overall thermal resistance between the stack and the free stream. This optimal number can be predicted by theory [equation (15)] and is validated by numerical simulations and laboratory measurements in the Re_L range 10^2–10^4 (Table 2).

(c) The scale of the minimum thermal resistance can be anticipated theoretically [equation (21)]. This scaling was used to construct a compact correlation [equation (22)].

(d) A stack with more plates than the optimal number can be modeled as a saturated porous medium with Darcy flow. The computations are faster and permit a study of the effect of the fluid/solid thermal conductivity ratio.

Acknowledgements—This work was supported by the IBM Corporation, Research Triangle Park, NC, and by a grant from the North Carolina Supercomputing Center.

REFERENCES

1. M. Hirata, Y. Kakita, Y. Yada, Y. Hirose, T. Morikawa and H. Enomoto, Temperature distribution of finned integrated circuits, *Fujitsu Sci. Tech. J.* **6**(4), 91–115 (1970).
2. W. Nakayama, H. Matsushima and P. Goel, Forced convective heat transfer from arrays of finned packages. In *Cooling Technology for Electronic Equipment* (Edited by W. Aung), pp. 195–210. Hemisphere, New York (1988).
3. H. Matsushima, T. Yanagida and Y. Kondo, Algorithm for predicting the thermal resistance of finned LSI packages mounted on a circuit board, *Heat Transfer Jap. Res.* **21**(5), 504–517 (1992).
4. A. Bar-Cohen and W. M. Rohsenow, Thermally optimum spacing of vertical, natural convection cooled, parallel plates, *J. Heat Transfer* **106**, 116–123 (1984).
5. S. H. Kim, N. K. Anand and L. S. Fletcher, Free convection between series of vertical parallel plates with embedded line heat sources, *J. Heat Transfer* **113**, 108–115 (1991).
6. N. K. Anand, S. H. Kim and L. S. Fletcher, The effect of plate spacing on free convection between heated parallel plates, *J. Heat Transfer* **114**, 515–518 (1992).
7. F. P. Incropera, Convection heat transfer in electronic equipment cooling, *J. Heat Transfer* **110**, 1097–1111 (1988).
8. G. P. Peterson and A. Ortega, Thermal control of electronic equipment and devices, *Adv. Heat Transfer* **20**, 181–314 (1990).
9. R. C. Schmidt and S. V. Patankar, A numerical study of laminar forced convection across heated rectangular blocks in two-dimensional ducts, ASME Paper No. 86-WA/HT-88 (1986).
10. J. Davalath and Y. Bayazitoglu, Forced convection cooling across rectangular blocks, *J. Heat Transfer* **109**, 321–328 (1987).
11. A. Bejan and E. Sciubba, The optimal spacing of parallel plates cooled by forced convection, *Int. J. Heat Mass Transfer* **35**, 3259–3264 (1992).
12. S. Mereu, E. Sciubba and A. Bejan, The optimal cooling of a stack of heat generating boards with fixed pressure drop, flowrate or pumping power, *Int. J. Heat Mass Transfer* **36**, 3677–3686 (1993).
13. A. Bejan and Al. M. Morega, The optimal spacing of a stack of plates cooled by turbulent forced convection, *Int. J. Heat Mass Transfer* **37**, 1045–1048 (1994).
14. A. Bejan, Al. M. Morega, S. W. Lee and S. J. Kim, The cooling of a heat generating board inside a parallel-plate channel, *Int. J. Heat Fluid Flow* **14**, 170–176 (1993).
15. Al. M. Morega and A. Bejan, Optimal spacing of parallel boards with discrete heat sources cooled by laminar forced convection, *Numer. Heat Transfer, Part A, Appl.* **25**, 373–392 (1994).
16. M. Morega and A. Bejan, Plate fins with variable thickness and height for air-cooled electronic modules, *Int. J. Heat Mass Transfer* **37**, Suppl. 1, 433–446 (1994).
17. National Instruments, *IEEE-488 and V × I Bus Control, Data Acquisition and Analysis* (1992).
18. S. Sasaki and T. Kishimoto, Optimal structure for microgrooved cooling fin for high-power LSI devices, *Electron. Lett.* **22**(25), 1332–1334 (1986).
19. *FIDAP Theoretical Manual and Examples Manual*, Revision 6.0. Fluid Dynamics International, Evanston, IL (April 1991).
20. C. A. J. Fletcher, *Computational Techniques for Fluid Dynamics* 2. *Specific Techniques for Different Flow Categories*, pp. 366–368. Springer, New York (1987).
21. N. Ashiwake, W. Nakayama and T. Daikoku, Forced convective heat transfer from LSI packages in an air-cooled wiring card array, *ASME HTD* **28**, 35–42 (1983).
22. A. Bejan, *Heat Transfer*, p. 324, problem 6.12. Wiley, New York (1993).
23. A. Bejan, *Convection Heat Transfer*, pp. 382–383, problem 3. Wiley, New York (1984).
24. D. A. Nield and A. Bejan, *Convection in Porous Media*, pp. 22–23. Springer, New York (1992).